Experimental study on the freezing/thawing characteristic curves of sand/clay mixtures

Quoc-Hung Vu, Anh Minh Tang, Jean-Michel Pereira

Experimental study on the freezing/thawing characteristic curves of sand/clay mixtures

Quoc-Hung Vu, Anh-Minh Tang & Jean-Michel Pereira

Laboratoire Navier, École des Ponts, Université Gustave Eiffel, CNRS, Marne-la-Vallée, France

ABSTRACT

The soil freezing characteristic curve (SFCC), relating temperature and unfrozen water content, is essential in modelling hydro-thermal processes in permafrost. In this study, the SFCC of sand/clay mixtures, with clay content varying from 0 to 20%, was determined. Compacted soil samples were first subjected to a freezing path (temperature decreasing from 0 °C to -3 °C) followed by a subsequent thawing path (temperature increasing from -3 °C to 0 °C). During this freezing/thawing cycle, volumetric unfrozen water content was measured as a function of soil temperature. The results show a significant hysteresis of the relationship between these two parameters. This finding is important because the hysteresis of SFCC is rarely considered in the modelling of hydro-thermal processes in permafrost. In addition, clear effects of clay content on the thawing curve were identified. At a given temperature, volumetric unfrozen water increases with clay content. Finally, a model predicting the SFCC of sandy soils was introduced, considering the effect of clay content.

1 INTRODUCTION

More than 20% of the world's land surface is underlain by permafrost, particularly in Russia, Canada and China (French 2007). With diverse human activities in cold regions such as mining, oil exploitation, construction, etc., freezing-thawing processes in frozen soils cause geotechnical engineering problems including damage to pavements and existing foundation structures, etc.

Frozen soil consists of mineral particles, liquid water, ice and gases (air and water vapour). The freezing process, when a fraction of liquid water solidifies into ice at temperatures sufficiently below 0 °C (Andersland and Ladanyi 1994), causes significant modifications of the physical-hydraulic-mechanical properties of soils (Andersland and Ladanyi 2004). The freezing-thawing process is usually the main cause of frost heave and thaw settlement inducing damages to infrastructure in permafrost of cold regions (Russo et al. 2015; Han et al. 2016; Zhang et al. 2016a; Yu et al. 2020). Interested readers are referred to Bordignon (2020) for a scientometric review of permafrost research with a focus on infrastructure vulnerability.

The Soil Freezing Characteristic Curve (SFCC) represents the relationship between the temperature and the quantity of liquid water in the soil. It is one of the most essential data in studying the hydro-thermal behaviour of permafrost. In general, the SFCC can be described using empirical models or derived from the Soil Water Retention Curve (SWRC) or a thermodynamic approach. In the first approach, different empirical models have been determined experimentally using power, piecewise or exponential functions (Anderson and Tice 1972; Tice et al. 1976; Ye et al. 2007; Kozlowski 2007; Ge et al. 2011; Kozlowski and Nartowska 2013; He et al. 2020; Teng et al. 2021). The second approach is based on the theoretical similarity between freezing-thawing and drying-wetting processes that is illustrated by Clausius-Clapeyron equation (Zhang et al. 2007, 2016b; Dall'Amico 2010; Sheshukov and Nieber 2011; Liu and Yu 2013; Zhou et al. 2019; Teng et al. 2020; Li and Vanapalli 2023). The two approaches capture the effects of supercooling, hysteresis, pore blocking, capillarity, free energy barriers, contact angles and electrolytes (Bittelli et al. 2003; Li et al. 2020). However, aside from a few models (e.g., Zhou et al. 2019), most of the existing SFCCs consider a unique relationship between unfrozen water content and temperature and ignore hysteresis effects (i.e., different paths between freezing and thawing).

SFCC can be determined in the laboratory by subjecting a soil specimen to a freeze-thaw cycle. Different methods can be used to measure unfrozen water content at negative temperatures such as dilatometry (Koopmans and Miller 1966; Patterson and Smith 1981), gas dilatometry (Spaans and Baker 1995), adiabatic calorimetry (Kolaian and Low 1963; Anderson and Tice 1973), isothermal calorimetry (Tice et al. 1976), differential scanning calorimetry (Yong et al. 1979; Kozlowski 2003, 2004), X-ray diffraction (Anderson and Hoekstra 1965; Anderson and Morgenstern 1973), time/frequency domain reflectometry (TDR/FDR; Stähli and Stadler 1997; Zhou et al. 2014; Schafer and Beier 2020) and pulsed nuclear magnetic resonance (P-NMR; Tice et al. 1981; Watanabe and Mizoguchi 2002; Li et al. 2020).

It is found that the shape of SFCC depends on several factors, including liquid limit (Tice et al. 1976), stress condition (Mu et al. 2019), salt content and solute types (Ming et al. 2020), initial water content or degree of saturation (Jia et al. 2019), types of soil (Zhang et al. 2020), and fines content (Tian et al. 2014). Among these factors, fines content can influence others (liquid limit, pore-size distribution and types of soil). As far as fines content is concerned, by determining the unfrozen water content of several clays, a silt and a gravel, Tice et al. (1976) observed significantly different unfrozen water contents at the same temperature below 0°C. Tian et al. (2014) carried out tests on three soils corresponding to three clay contents and found that the unfrozen water degree of saturation also changed in different ways in both freezing and thawing processes. For soils containing higher clay fraction, unfrozen water degree of saturation was higher at any given

temperature below the freezing point and the hysteresis loop was smaller.

The present study aims to investigate the effects of clay content on the SFCC of sandy soils. Sandy soils with clay content of 0, 5, 10, 15, and 20% were compacted and saturated. The specimens were then subjected to freezing and thawing paths in undrained conditions. During this freezing-thawing cycle, the soil's temperature and unfrozen water content were measured.

2 MATERIALS AND EXPERIMENTAL METHODS

2.1 Materials

Fontainebleau sand and Speswhite kaolin clay (physical properties shown in Table 1) were mixed in a dry state, using an automatic mixer, to obtain five sand/clay mixtures with different clay contents varying from 0 to 20%. The two materials were chosen because their hydro-mechanical properties have been widely investigated (Boussaid 2005). Figure 1 shows the grain size distribution curves of the five mixtures: S0, S5, S10, S15, and S20 (e.g., S10 corresponds to 10% of clay and 90% of sand in dry mass). Then, distilled water was added to the mixtures to reach their optimum water content, as determined from the Standard Proctor compaction curve obtained for the same soil compositions (Boussaid 2005). Wet soil was finally left to equilibrate in a plastic bag for at least 24 hours before compaction in a cylindrical cell using a Proctor rammer to the maximum dry density. The tested soil properties are shown in Table 2.

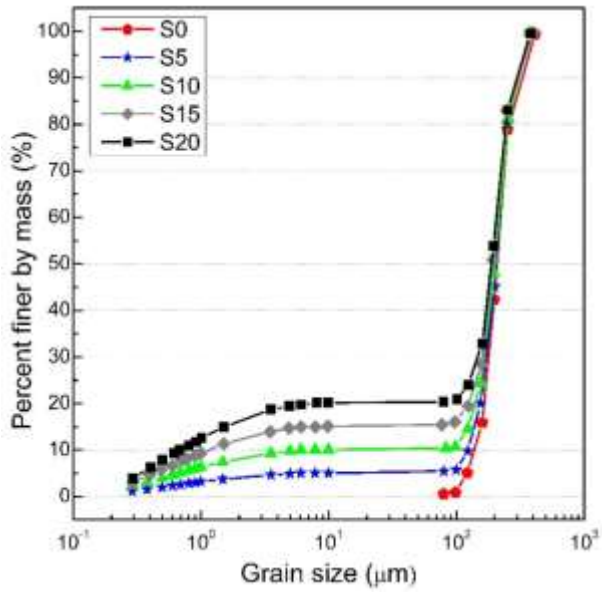

Figure 1. Grain size distribution curves of the five mixtures.

2.2 Experimental setup and procedure

The experimental setup is shown in Figure 2. A soil specimen was confined in a rigid metallic cylindrical cell (150 mm in height and 150 mm in diameter). Four sensors measuring the soil thermal conductivity (KD2-Pro), suction (T5x), temperature (PT100) and water content (ThetaProbe ML2x) were installed. The cell was submerged in a temperature-controlled bath (F38-EH JULABO with ±0.03 °C in accuracy). As Thetaprobe sensor measures soil apparent dielectric constant (K_a) which is the ratio of the dielectric permittivity of a substance to that of vacuum, soil volumetric unfrozen water content (θ_w) was estimated from the measured K_a by using empirical Equation 1 (Smith and Tice 1988) and Equation 2 (Topp et al. 1980) for frozen and unfrozen soils, respectively. Equation 1 was used where ice is expected to exist in soil (i.e., after the occurrence of freezing and before the completion of thawing). Equation 2 was used only for the initial state (before any freezing) and for the final state where thawing is complete.

Table 1. Physical properties of Speswhite kaolin clay and Fontainebleau sand (Boussaid 2005).

Property	Speswhite kaolin clay	Fontainebleau sand
Median grain size, $\boldsymbol{D_{50}}$ (mm)	-	0.21
Uniformity coefficient, $\boldsymbol{C_U}$	-	1.52
Minimum void ratio, $\boldsymbol{e_{min}}$	-	0.54
Maximum void ratio, $\boldsymbol{e_{max}}$	-	0.94
Particle density, $\boldsymbol{\rho_{soslid}}$ (Mg/m³)	2.65	2.65
Minimum dry density, $\boldsymbol{\rho_{d,min}}$ (Mg/m³)	-	1.37
Maximum dry density, $\boldsymbol{\rho_{d,max}}$ (Mg/m³)	1.45	1.72
Liquid limit, $\boldsymbol{LL}$ (%)	55	-
Plastic limit, $\boldsymbol{PL}$ (%)	30	-
Plasticity index, $\boldsymbol{PI}$	25	-
Specific surface area (m²/g)	0.94	-
Particles diameter < 0.002 mm (%)	79	-
Particles diameter > 0.01 mm (%)	0.5	-

Table 2. Physical properties of tested soils.

Test No.	Clay content (%)	Water content at compaction (%)	Dry density, $\boldsymbol{\rho_d}$ (Mg/m³)	Porosity, $\boldsymbol{n}$ (-)
S20	20	11.2	1.98	0.25
S15	15	9.1	1.99	0.25
S10	10	8.0	1.91	0.28
S5	5	7.0	1.78	0.33
S0	0	5.6	1.67	0.37

$$\theta_u = -0.1458 + 3.868 \times 10^{-2} \times K_a - 8.502 \times 10^{-4} \times K_a^2 + 9.92 \times 10^{-6} \times K_a^3 \quad (1)$$

$$\theta_u = -5.3 \times 10^{-2} + 2.92 \times 10^{-2} \times K_a - 5.5 \times 10^{-4} \times K_a^2 + 4.3 \times 10^{-6} \times K_a^3 \quad (2)$$

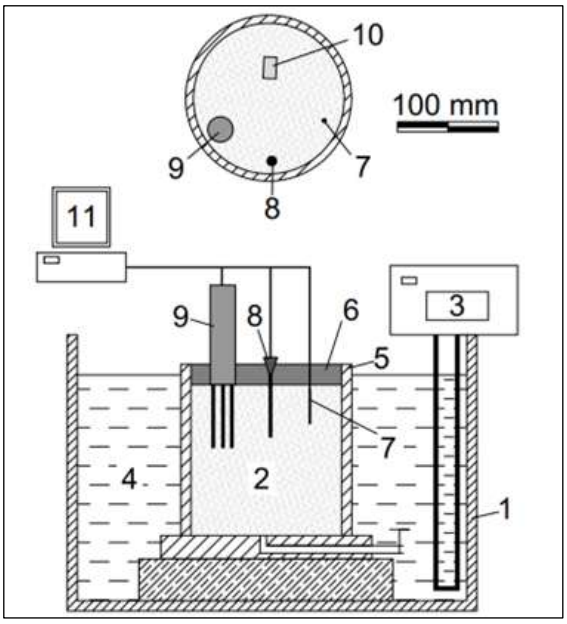

Figure 2. Schematic view of the experimental setup (Vu et al. 2022).

Table 3. Properties of sensors used in the experiments.

Measured variable	Method	Accuracy	Range
Temperature	Resistance temperature detector	±0.03 °C	-200 to 400 °C
Volumetric unfrozen water content	Time domain reflectometry (dielectric constant)	0.01 m^3/m^3	0.01 to 1 m^3/m^3

After the installation of the sensors, an insulating cover made of expanded polystyrene was placed over the experimental setup to avoid heat exchange with ambient air. Then, the soil specimen was saturated by injecting water from the bottom of the specimen for 0.5 to 2 days depending on the clay content (a longer duration was required for samples with higher clay content and thus lower hydraulic conductivity). The whole system was then transferred inside the temperature-controlled bath (Figure 2). The bath temperature was first set at a temperature between 0 °C and -1 °C (slightly higher than the expected spontaneous nucleation temperature which marks the freezing process). The start of each test began with a temperature decrease from -1 °C towards -3 °C, before a temperature increase later in the test. The bath temperature was decreased in steps of 0.1 °C to freeze the soil pore water. Each temperature ramp took less than one hour to stabilize and it was held constant for several hours. Once the freezing was triggered, the temperature continued to be decreased in steps of 0.2 °C until -2 °C or -3 °C to observe the change of liquid water content during further cooling. Afterwards, during the warming path, the bath temperature was increased in steps of 0.2 °C until 0 °C to thaw the frozen soil. During both cooling and warming paths, the bath temperature was changed to the subsequent step only when soil temperature and volumetric unfrozen water content had reached an equilibrium state, considered achieved when these two quantities did not change (< 0.05 °C for temperature and < 1% for water content) during at least 2 h.

3 EXPERIMENTAL RESULTS

As an example, the results of test S10 are shown in Figure 3 where soil temperature and unfrozen water content are plotted versus elapsed time for the whole freezing and thawing path.

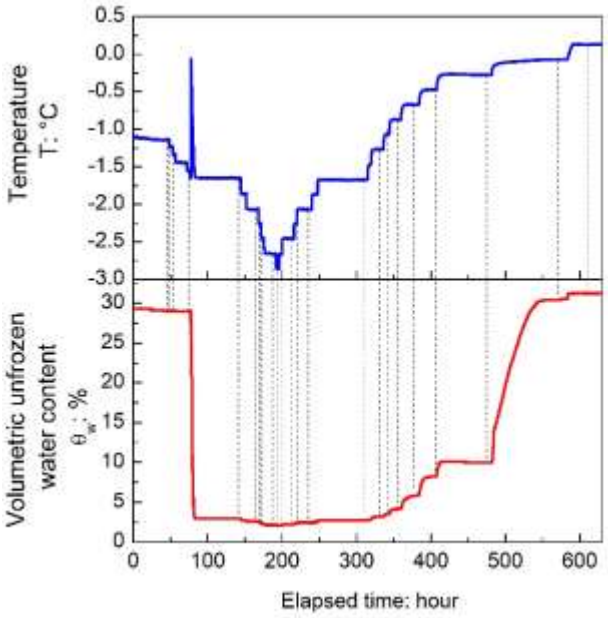

Figure 3. Soil temperature and volumetric unfrozen water content versus elapsed time of test S10.

From -1.2 °C, soil temperature was decreased in steps of 0.1 °C down to -1.6 °C. During this stage, soil temperature was controlled through the bath's temperature, and volumetric water content remained constant. When soil temperature reached -1.6 °C, soil freezing started inducing abrupt changes in the soil temperature. The latter increased abruptly to -0.1 °C before a progressive decrease and reached the imposed temperature (-1.6 °C) again while soil water content decreased to 3%. These results are representative of the freezing process because transformation of liquid water to ice releases latent heat (Vu et al. 2022). After the freezing process, a decrease in temperature induced a slight decrease in volumetric unfrozen water content. During the warming path, temperature was increased by steps of 0.2 °C from -2.8 °C to 0 °C. It induced thawing of frozen water (corresponding to a gradual increase of unfrozen water content when compared to the freezing case).

From the results shown in Figure 3, volumetric unfrozen water content obtained at the end of each step is plotted versus the corresponding soil temperature for test S10 in Figure 4. The hysteresis, which is clearly shown in Figure 4, is significant in the temperature range of -0.1 °C to -1.6 °C.

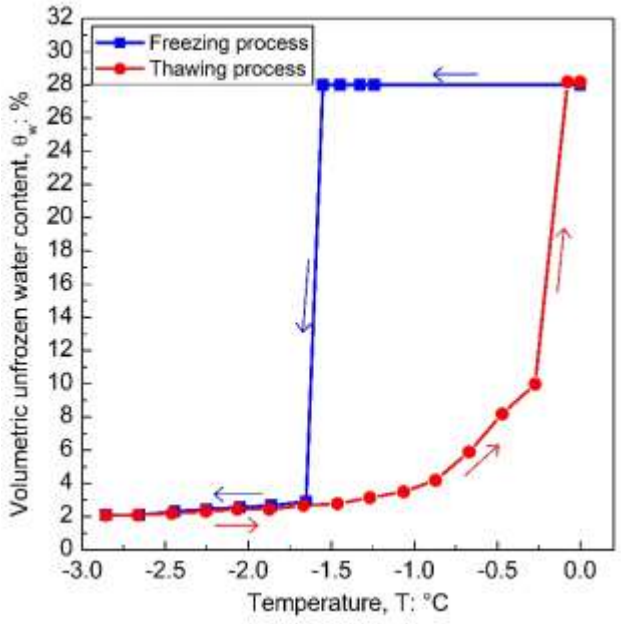

Figure 4. Soil freeing characteristic curve determined from test S10.

SFCC of all soils are plotted in Figure 5 where unfrozen water degree of saturation is plotted as a function of temperature for the thawing path. The freezing path is not analysed in this study because it depends on other factors (besides clay content) such as the test procedure. The results show that the unfrozen water degree of saturation increased gradually with thawing.

4 SFCC MODEL OF SANDY SOILS

Van Genuchten's model, which is initially proposed for the water retention curve in unsaturated unfrozen soil, allows relating cryogenic suction (*s*) to unfrozen water content in frozen soil as shown in Equation 3 (van Genuchten 1980; Nishimura et al. 2009):

$$S_w = \left[1 + \left(\frac{s}{\rho_r}\right)^{\frac{1}{1-\lambda_r}}\right]^{-\lambda_r} \quad (3)$$

where:

- S_w is the unfrozen water degree of saturation.
- λ_r is a fitting parameter which relates to the curvature at temperatures close to 0 °C.
- ρ_r is a fitting parameter (kPa) corresponding to the soil suction at which the residual unfrozen degree of saturation is reached. For larger values of suction, the unfrozen degree of saturation changes insignificantly.
- s is the soil suction (kPa).

To relate the temperature and soil suction, the Clausius-Clapeyron equation was used to estimate suction during thawing as follows:

$$s = L_f \rho_w \frac{T - T_f}{T_f} \quad (4)$$

where $\rho_w = 1000$ kg/m^3 is the density of water, $L_f = 334$ kJ/kg is the latent heat of fusion, $T_f = 273.15$ K is the freezing point of water, T is the soil temperature in Kelvin.

Based on the results from the thawing path in tests S0 to S20, van Genuchten model for SFCC for different soils was calibrated as shown in Figure 5. The two fitting parameters for each soil are shown in Table 4. The effect of clay content on fitting parameters of van Genuchten's model is shown in Figure 6.

Table 4: van Genuchten's model parameters.

Materials	Fitting parameter $\boldsymbol{\lambda_r}$(-)	Fitting parameter $\boldsymbol{\rho_r}$(kPa)
S0	0.46	30
S5	0.46	98
S10	0.44	126
S15	0.37	140
S20	0.33	150

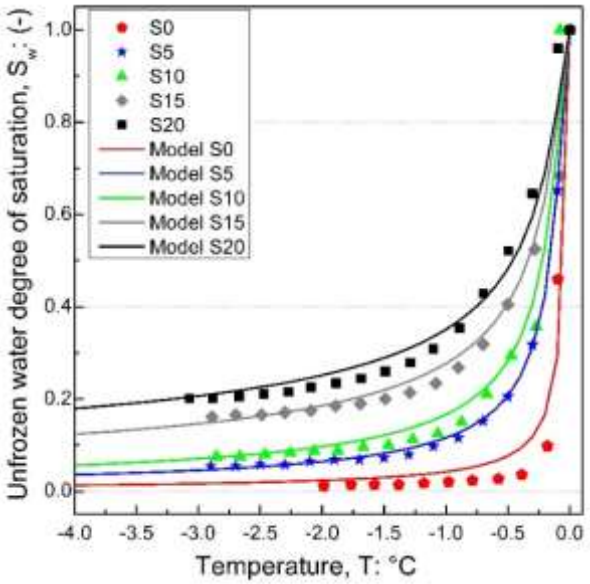

Figure 5. van Genuchten hydraulic model fitted to experimental SFCC (thawing path).

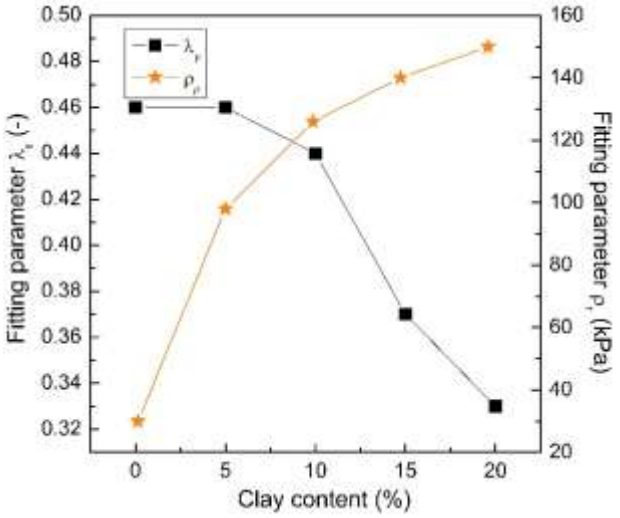

Figure 6: Effect of clay content on fitting parameters of van Genuchten's model.

5 DISCUSSION

In this study, to determine the relationship between unfrozen water content and temperature during a freezing-thawing cycle, large soil specimens (150 mm in height and 150 mm in diameter) were prepared to embed several sensors within the soil mass without interference between sensors. To minimise thermal and any other gradients, soil temperature was changed by small steps and equilibrium was checked at the end of each step prior the subsequent step. At equilibrium, the soil temperature and unfrozen water content were thus supposed to be homogeneous within the specimen.

The measurement of unfrozen water content in the present study was obtained from the measurement of the apparent dielectric constant, K_a, which is strongly dependent of temperature (Wraith and Or 1999; Haynes 2016). In this study, Topp's empirical model (Equation 2) is used for its better compatibility with unfrozen soils in comparison to the existing models in the literature (Topp et al. 1980; Roth et al. 1990; Stähli and Stadler 1997; Schafer and Beier 2020). For frozen soils, Smith and Tice (1988) proposed a model based on a comparison of unfrozen water content for 25 soils covering a wide range of specific surface areas. For this reason, in the present work, the model of Smith and Tice (1988; equation 1), which provides an accuracy of ±3%, compared to experimental data, was used for frozen soils.

Residual unfrozen water degree of saturation (value corresponding to lowest temperature in Figure 5) was observed to increase with clay content. Increasing clay content induces an increase in the amount of specific surface of soils (Tian et al. 2014). When freezing is triggered, only free water is frozen (Bing and Ma 2011). Residual unfrozen water should then correspond to bound water. According to Tian et al. (2014), the amount of bound water in soils is proportional to the thickness of the electric double layer and the specific surface area. In the present study, a higher clay content corresponds to a higher specific surface area and an associated increase in bound water.

Hysteresis of SFCC (difference between the freezing and the thawing curves) is usually attributed to the same factors inducing hysteresis in SWCC, such as the effect of electrolytes, pore geometry, pore blocking, effect of contact angle and change in pore structure (Ren and Vanapalli 2019). In this study, the hysteresis was observed only above the temperature of spontaneous nucleation (at -1.6 °C for the test S10). Supercooling, the process of lowering the temperature of a liquid below its freezing point without phase change, could mainly contribute to hysteresis due to the absence of electrolytes.

Figure 5 demonstrates a significant effect of clay content on the thawing path of SFCC. Actually, at a given temperature, a higher unfrozen water degree of saturation was obtained at a higher clay content. These results are consistent with the findings of previous works (Tice et al. 1976; Tian et al. 2014; Zhang et al. 2020; Li et al. 2020). Following these studies, Gibbs-Thompson equation which presents the thermodynamic treatment of the solid/liquid transition in confined pores can be used to relate the pore size distribution and the thawing path of SFCC; a lower temperature corresponds to a smaller pore (Vu et al. 2023). In this study, soil having higher clay content would have a larger volume of micropores (inter-aggregates and intra-aggregates pores) and consequently a lower volume of macropores (space between sand particles).

van Genuchten model with two parameters corresponding to the residual unfrozen water degree of saturation and the curvature at temperatures close to 0 C can predict well the SFCC of sandy soils with varying clay content in the thawing path. However, the hysteresis could not be captured by the model as well as the existing models in literature due to the abrupt decrease of unfrozen water degree of saturation at freezing temperature along the freezing path.

The results of this work reveal the role of fines content on soil freezing characteristic curve. Results shown in Figure 6 would help to better choose parameters of van Genuchten's model when clay fines content is known.

6 CONCLUSIONS

The results obtained in this study show that clay content in sandy soils significantly influenced the SFCC along the thawing path. The freezing path was not presented because it is influenced by other factors such as the test procedure. Based on the investigation of five levels of clay content (varying from 0 to 20%), the following conclusions can be drawn:

- The hysteresis of SFCC in sandy soils is mainly due to supercooling.

- The SFCC along a thawing path is significantly influenced by clay content.
- The SFCC along the thawing path of five soils with increasing clay content from 0% to 20% can be well predicted by van Genuchten model. The model could not capture SFCC in freezing path due to an abrupt change of unfrozen water content at freezing temperature.

7 REFERENCES

Andersland, O.B. and Ladanyi, B. 1994. 'An Introduction to Frozen Ground Engineering', in *An Introduction to Frozen Ground Engineering*. Springer Science & Business Media.

Andersland, O.B. and Ladanyi, B. 2004. *Frozen Ground Engineering*. John Wiley & Sons.

Anderson, D.M.and Hoekstra, P. 1965. 'Migration of interlamellar water during freezing and thawing of Wyoming bentonite', *Soil Science Society of America Journal* 29(5), pp. 498–504. doi:10.2136/sssaj1965.03615995002900050010x.

Anderson, D.M. and Morgenstern, N.R. 1973. 'Physics, chemistry, and mechanics of frozen ground: a review', in *Permafrost: North American Contribution [to The] Second International Conference*. Washington, DC, United States.

Anderson, D.M. and Tice, A.R. 1972. 'Predicting unfrozen water contents in frozen soils from surface area measurements', *Highway Research Record* 393(2), pp. 12–18.

Anderson, D.M. and Tice, A.R. 1973. 'The unfrozen interfacial phase in frozen soil water systems', in A. Hadas, D. Swartzendruber, P.E. Rijtema, M. Fuchs and B. Yaron (eds.), *Physical aspects of soil water and salts in ecosystems*. Heidelberg, Germany: Springer-Verlag Berlin Heidelberg, pp. 107–124.

Bing, H. and Ma, W. 2011. 'Laboratory investigation of the freezing point of saline soil', *Cold Regions Science and Technology* 67(1–2), pp. 79–88. doi:10.1016/j.coldregions.2011.02.008.

Bittelli, M., Flury, M., and Campbell, G.S. 2003. 'A thermodielectric analyzer to measure the freezing and moisture characteristic of porous media', *Water Resources Research* 39(2).

Bordignon, F. 2021. 'A scientometric review of permafrost research based on textual analysis (1948–2020)', *Scientometrics* 126, pp. 417–436. doi:10.1007/s11192-020-03747-4.

Boussaid, K. 2005. *Sols intermédiaires pour la modélisation physique : application aux fondations superficielles*. PhD thesis, École Centrale de Nantes et Université de Nantes.

Dall'Amico, M. 2010. *Coupled water and heat transfer in permafrost modeling*. PhD thesis, Faculty of Engineering, University of Trento.

French, H.M. 2007. *The periglacial environment*. Third Edition. John Wiley & Sons.

Ge, S., McKenzie, J., Voss, C., and Wu, Q. 2011. 'Exchange of groundwater and surface-water mediated by permafrost response to seasonal and long term air temperature variation', *Geophysical Research Letters* 38(14), pp. 1–6. doi:10.1029/2011GL047911.

Van Genuchten, M.Th. 1980. 'A Closed-form Equation for Predicting the Hydraulic Conductivity of Unsaturated Soils', *Soil Science Society of America Journal* 44(5), pp. 892–898. doi:10.2136/sssaj1980.03615995004400050002x.

Han, L., Ye, G., Li, Y., Xia, X., and Wang, J. 2016. 'In situ monitoring of frost heave pressure during cross passage construction using ground-freezing method', *Canadian Geotechnical Journal* 53(3), pp. 530–539. doi:10.1139/cgj-2014-0486.

Haynes, W.M. (ed.) 2016. *CRC Handbook of Chemistry and Physics*. 97th edition. Boca Raton, Florida, United States: CRC press.

He, Z., Teng, J., Yang, Z., Liang, L., Li, H., and Zhang, S. 2020. 'An analysis of vapour transfer in unsaturated freezing soils', *Cold Regions Science and Technology* 169(68), 102914. doi:10.1016/j.coldregions.2019.102914.

Jia, H., Ding, S., Wang, Y. et al. 2019. 'An NMR-based investigation of pore water freezing process in sandstone', *Cold Regions Science and Technology* 168, 102893. doi:10.1016/j.coldregions.2019.102893

Kolaian, J.H. and Low, P.F. 1963. 'Calorimetric determination of unfrozen water in montmorillonite pastes', *Soil Science* 95(6), pp. 376–384.

Koopmans, R.W.R. and Miller, R.D. 1966. 'Soil freezing and soil water characteristic curves', *Soil Science Society of America Journal* 30(6), pp. 680–685.

Kozlowski, T. 2003. 'A comprehensive method of determining the soil unfrozen water curves', *Cold Regions Science and Technology* 36(1–3), pp. 71–79. doi:10.1016/S0165-232X(03)00007-7.

Kozlowski, T. 2004. 'Soil freezing point as obtained on melting', *Cold Regions Science and Technology* 38(2–3), pp. 93–101. doi:10.1016/j.coldregions.2003.09.001.

Kozlowski, T. 2007. 'A semi-empirical model for phase composition of water in clay–water systems', *Cold Regions Science and Technology* 49(3), pp. 226–236. doi:10.1016/j.coldregions.2007.03.013.

Kozlowski, T. and Nartowska, E. 2013. 'Unfrozen Water Content in Representative Bentonites of Different Origin Subjected to Cyclic Freezing and Thawing', *Vadose Zone Journal* 12(1). doi:10.2136/vzj2012.0057.

Li, Z., Chen, J., and Sugimoto, M. 2020. 'Pulsed NMR Measurements of Unfrozen Water Content in Partially Frozen Soil', *Journal of Cold Regions Engineering* 34(3), 04020013. doi:10.1061/(ASCE)CR.1943-5495.0000220.

Liu, Z. and Yu, X. 2013. 'Physically Based Equation for Phase Composition Curve of Frozen Soils', *Journal of the Transportation Research Board* 2349(1), pp. 93–99. doi:10.3141/2349-11.

Li, Y. and Vanapalli, S.K. 2023. 'Equations for soil freezing characteristics curves based on the thermodynamics principles', *Geoderma* 439, 11644. doi:10.1016/j.geoderma.2023.116644

Ming, F., Chen, L., Li, D. and Du, C. 2020. 'Investigation into freezing point depression in soil caused by NaCl solution', *Water* 12, 2232. doi:10.3390/w12082232

Mu, Q.Y., Zhou, C., Ng. C.W.W., and Zhou, G.G.D. 2019. 'Stress effects on soil freezing characteristic curve: equipment development and experimental results', *Vadose Zone Journal* 18(1), pp.1–10. doi:10.2136/vzj2018.11.0199

Nishimura, S., Gens, A., Olivella, S., and Jardine, R.J. 2009. 'THM-coupled finite element analysis of frozen soil: Formulation and application', *Geotechnique* 59(3), pp. 159–171. doi:10.1680/geot.2009.59.3.159.

Patterson, D.E. and Smith, M.W. 1981. 'The measurement of unfrozen water content by time domain reflectometry: results from laboratory tests', *Canadian Geotechnical Journal* 18(1), pp. 131–144. doi:10.1139/t81-012.

Ren, J. and Vanapalli, S.K. 2019. 'Comparison of Soil-Freezing and Soil-Water Characteristic Curves of Two Canadian Soils', *Vadose Zone Journal* 18(1), pp. 1–14. doi:10.2136/vzj2018.10.0185.

Roth, K., Schulin, R., Fluhler, H., and Attinger, W. 1990. 'Calibration of time domain reflectometry for water content measurement using a composite dielectric approach', *Water Resources Research*, 26(10), pp. 2267–2273.

Russo, G., Corbo, A., Cavuoto, F., and Autuori, S. 2015. 'Artificial Ground Freezing to excavate a tunnel in sandy soil. Measurements and back analysis', *Tunnelling and Underground Space Technology* 50, pp. 226–238. doi:10.1016/j.tust.2015.07.008.

Schafer, H. and Beier, N. 2020. 'Estimating soil-water characteristic curve from soil-freezing characteristic curve for mine waste tailings using time domain reflectometry', *Canadian Geotechnical Journal* 57(1), pp. 73–84. doi:10.1139/cgj-2018-0145.

Sheshukov, A.Y. and Nieber, J.L. 2011. 'One-dimensional freezing of nonheaving unsaturated soils: Model formulation and similarity solution', *Water Resources Research* 47(11), pp. 1–17. doi:10.1029/2011WR010512.

Smith, M.W. and Tice, A.R. 1988. 'Measurement of the unfrozen water content of soils: comparison of NMR and TDR methods', *Cold Regions Research and Engineering Laboratory* CRREL Report 88-18.

Spaans, E.J.A and Baker, J.M. 1995. 'Examining the use of time domain reflectometry for measuring liquid water content in frozen soil', Water Resources Research 31(12), pp. 2917–2925. doi:10.1029/95WR02769.

Stähli, M. and Stadler, D. 1997. 'Measurement of water and solute dynamics in freezing soil columns with time domain reflectometry', *Journal of Hydrology* 195(1–4), pp. 352–369. doi:10.1016/S0022-1694(96)03227-1.

Teng, J., Kou, J., Yan, X., Zhang, S., and Sheng, D. 2020. 'Parameterization of soil freezing characteristic curve for unsaturated soils', *Cold Regions Science and Technology* 170(68), 102928. doi:10.1016/j.coldregions.2019.102928.

Teng, J., Zhong, Y., Zhang, S., and Sheng, D. 2021. 'A mathematic model for the soil freezing characteristic curve: the roles of adsorption and capillarity', *Cold Regions Science and Technology* 181(68), 103178. doi:10.1016/j.coldregions.2020.103178.

Tian, H., Wei, C., Wei, H., and Zhou, J. 2014. 'Freezing and thawing characteristics of frozen soils: Bound water content and hysteresis phenomenon', *Cold Regions Science and Technology* 103, pp. 74–81. doi:10.1016/j.coldregions.2014.03.007.

Tice, A.R., Anderson, D.M., and Banin, A. 1976. 'The prediction of unfrozen water contents in frozen soils from liquid limit determinations', Cold Regions Research and Engineering Laboratory CRREL Report 76-8.

Tice, A.R., Anderson, D.M., and Sterrett, K.F. 1981. 'Unfrozen water contents of submarine permafrost determined by nuclear magnetic resonance' *Engineering Geology* 18(1–4), pp. 135–146.

Topp, G.C., Davis, J.L., and Annan, A.P. 1980. 'Electromagnetic determination of soil water content: Measurements in coaxial transmission lines', *Water Resources Research* 16(3), pp. 574–582.

Vu, Q.H., Pereira, J.M., and Tang, A.M. 2022. 'Effect of fines content on soil freezing characteristic curve of sandy soils', *Acta Geotechnica* 17(11), pp. 4921–4933. Springer Berlin Heidelberg. doi:10.1007/s11440-022-01672-9.

Vu, Q.H., Pereira, J.M., and Tang, A.M. 2023. 'Water retention curve of clayey sands determined from pore structure by using various methods', *E3S Web of Conferences* 382, 09006. Available at: https://doi.org/10.1051/e3sconf/202338209006.

Watanabe, K. and Mizoguchi, M. 2002. 'Amount of unfrozen water in frozen porous media saturated with solution', *Cold Regions Science and Technology* 34(2), pp. 103–110. doi:10.1016/S0165-232X(01)00063-5.

Wraith, J.M. and Or, D. 1999. 'Temperature effects on soil bulk dielectric permittivity measured by time domain reflectometry: Experimental evidence and hypothesis development', *Water Resources Research* 35(2), pp. 361–369.

Ye, M., Pan, F., Wu, Y.-S., Hu, B.X., Shirley, C., and Yu, Z. 2007. 'Assessment of radionuclide transport uncertainty in the unsaturated zone of Yucca Mountain', *Advances in Water Resources* 30(1), pp. 118–134. doi:10.1016/j.advwatres.2006.03.005.

Yong, R.N., Cheung, CH., and Sheeran, D.E. 1979. 'Prediction of Salt Influence on Unfrozen Water Content in Frozen Soils', *Engineering Geology* 13(1–4), pp. 137–155.

Yu, W., Zhang, T., Lu, Y., Han, F., Zhou, Y., and Hu, D. 2020. 'Engineering risk analysis in cold regions: State of the art and perspectives', *Cold Regions Science and Technology* 171(December 2019), 102963. doi:10.1016/j.coldregions.2019.102963.

Zhang, H., Zhang, J., Zhang, Z., Zhang, M., and Cao, W. 2020. 'Variation behavior of pore-water pressure in warm frozen soil under load and its relation to deformation', *Acta Geotechnica* 15(3), pp. 603–614.doi:10.1007/s11440-018-0736-4.

Zhang, S., Sheng, D., Zhao, G., Niu, F., and He, Z. 2016a. 'Analysis of frost heave mechanisms in a high-speed railway embankment', *Canadian Geotechnical Journal* 53(3), pp. 520–529. doi:10.1139/cgj-2014-0456.

Zhang, S., Teng, J., He, Z., Liu, Y., Liang, S., Yao, Y., and Sheng, D. 2016b. 'Canopy effect caused by vapour transfer in covered freezing soils', *Géotechnique* 66(11), pp. 927–940. doi:10.1680/jgeot.16.P.016.

Zhang, X., Sun, S.F., and Xue, Y. 2007. 'Development and Testing of a Frozen Soil Parameterization for Cold Region Studies', *Journal of Hydrometeorology* 8(4), pp. 690–701. doi:10.1175/JHM605.1.

Zhou, X., Zhou, J., Kinzelbach, W., and Stauffer, F. 2014. 'Simultaneous measurement of unfrozen water content and ice content in frozen soil using gamma ray attenuation and TDR', *Journal of the American Water Resources Association* 5(3), 2–2. doi:10.1111/j.1752-1688.1969.tb04897.x.

Zhou, Y., Zhou, J., Shi, X., and Zhou, G. 2019. 'Practical models describing hysteresis behavior of unfrozen water in frozen soil based on similarity analysis', *Cold Regions Science and Technology* 157, pp. 215–223. doi:10.1016/j.coldregions.2018.11.002.